EUROPEAN SYNCHROTRON RADIATION FACILITY

INSTALLATION EUROPEENNE DE RAYONNEMENT SYNCHROTRON

ESRF

Experiment Report Form

The double page inside this form is to be filled in by all users or groups of users who have had access to beam time for measurements at the ESRF.

Once completed, the report should be submitted electronically to the User Office via the User Portal:
https://wwws.esrf.fr/misapps/SMISWebClient/protected/welcome.do

Deadlines for submission of Experimental Reports

Experimental reports must be submitted within the period of 3 months after the end of the experiment.

Experiment Report supporting a new proposal ("relevant report")

If you are submitting a proposal for a new project, or to continue a project for which you have previously been allocated beam time, you must submit a report on each of your previous measurement(s):

- even on those carried out close to the proposal submission deadline (it can be a *"preliminary report"),*
- even for experiments whose scientific area is different form the scientific area of the new proposal,
- carried out on CRG beamlines.

You must then register the report(s) as "relevant report(s)" in the new application form for beam time.

Deadlines for submitting a report supporting a new proposal

- 1st March Proposal Round - **5th March**
- 10th September Proposal Round - **13th September**

The Review Committees reserve the right to reject new proposals from groups who have not reported on the use of beam time allocated previously.

Reports on experiments relating to long term projects

Proposers awarded beam time for a long term project are required to submit an interim report at the end of each year, irrespective of the number of shifts of beam time they have used.

Published papers

All users must give proper credit to ESRF staff members and proper mention to ESRF facilities which were essential for the results described in any ensuing publication. Further, they are obliged to send to the Joint ESRF/ ILL library the complete reference and the abstract of all papers appearing in print, and resulting from the use of the ESRF.

Should you wish to make more general comments on the experiment, please note them on the User Evaluation Form, and send both the Report and the Evaluation Form to the User Office.

Instructions for preparing your Report

- fill in a separate form for each project or series of measurements.
- type your report in English.
- include the experiment number to which the report refers.
- make sure that the text, tables and figures fit into the space available.
- if your work is published or is in press, you may prefer to paste in the abstract, and add full reference details. If the abstract is in a language other than English, please include an English translation.

ESRF	Experiment title: Peierls instability and Kohn anomaly in BaVS3	**Experiment number**: HC 4039
Beamline: ID28	**Date of experiment**: from:14/11/2018 to: 20/11/2018	**Date of report**: 09/03/2021
Shifts:18	**Local contact(s)**: Alexei Bosak	*Received at ESRF:*

Names and affiliations of applicants (* indicates experimentalists):

Adrien Girard

BOSAK Alexei *

ILAKOVAC Vita *

Pascale Foury-Leylekian *

WINKLER Bjoern

STEKIEL Michal

Report:

Single crystals of BaVS3, of a needlelike shape along the [001] axis, were grown by the tellurium flux method and studied.They were slightly polished to obtain lateral dimensions ofabout 100 μm in order to maximize the IXS signal and then mounted on a glass fiber and fixed with an epoxy glue. x-ray DS experiments were conducted first with the diffractometer built as a side station at the ID28, with a monochromatic beam of 17.8-keV photons. The DS maps were recorded with a Pilatus 3 X 1M detector in the range 30–300 K. Closed-cycle cryocooler with Kapton windows was used for both IXS and DS measurement. In the case ofDS data collection, an internal screen was added, which was rotating in opposite direction relatively to the cryostat movement. It allowed us to suppress the background scattering from both entrance and exit windows. The IXS experiments were conducted at the ID28 beamline of the ESRF, with the high-resolution spectrometer operating at an energy of 17.8 keV. With our setup, the energy resolution was about 3 meV. Acorrection of 10 K (14 K) is applied in IXS (DS) scans in orderto match the temperature of the structural transition with the MI transition determined by conductivity measurements, 69 K. Scattering angle restrictions imposed the choice of representative DS reconstruction as (h,k,3.5). However, different mount allowed us to explore essentially equivalent (h,k,4.5) plane by IXS, thus gaining the intensity. CrysAlis software (Rigaku–Oxford Diffraction) was used for the preliminarydiffraction data reconstructions. High-quality reconstructionswere performed with locally developed software.

1 - Thermal diffuse scattering

The reconstruction of the (h,0,l) plane of BaVS3, measured at 114 K is shown Fig.1(a).At l=n+1/2, it shows diffuse streaks extending in a∗ direction. They correspond to a hexagonal, honeycomb-shaped diffusion, visible already at RT in the reconstruction of the (h,k,3.5) plane [seeFig.1(b)]. At low temperature, when approaching TP from above, it disappears and is replaced by a diffuse-scattering spot-pattern which condenses in superstructure satellites at TP, see Figs.1(c)–2(e). Note that the intensity range of the DS taken at low temperature is modified relatively to this at 300 K, in order to make the diffusion pattern more visible. The intensity of the honeycomb-shaped diffusion, as measured at the A'point (diffuse hexagon corner), underlines all important changes in BaVS3. When lowering the temperature, it

increases at the orthorhombic transition (TS), strongly decreases at the minimum of resistivity (Tm) and progressively vanishesbelow the Peierls transition (TP). The reduced wave vector of the superstructure satellites [see Fig.1(e)] appearing at TP is (0.5, 0, 0.5) in hexagonal settings (space group P63/mmc). This correspond to the point L of the first Brillouin zone (BZ), as shown by black points in Fig.1(g). Other satellites are equivalent due to the symmetry operations of the P63/mmc space group. One third of them are located at the diffuse hexagon edge, and are indicated by open circles in Fig.1(g)(L'points). Hexagon-shaped diffusion is observed in (h,k, 3.5) and (h,k, 4.5) planes. But it is not visible in the (h,k, 2.5) plane (not shown), where only diffuse spots appear at satellites positions above TP. The increase of the hexagonal DS intensity with l shows that the scattering is of displacive nature, with a pre-dominantly c (z) direction of atomic displacement. In order to understand the origin of the diffuse hexagons, we performed lattice dynamics calculation within density-functional theory(DFT) implemented in the CASTEP code. TDS-map calculationof the (h,k, 3.5) plane in the Cmc21 space group is shown Fig.1(f).The calculation shows that the TDS is a result of phonons of an energy of about 6–9 meV, due mostly to an out of phase motion in the z direction of the two Ba ions in the unit cell.

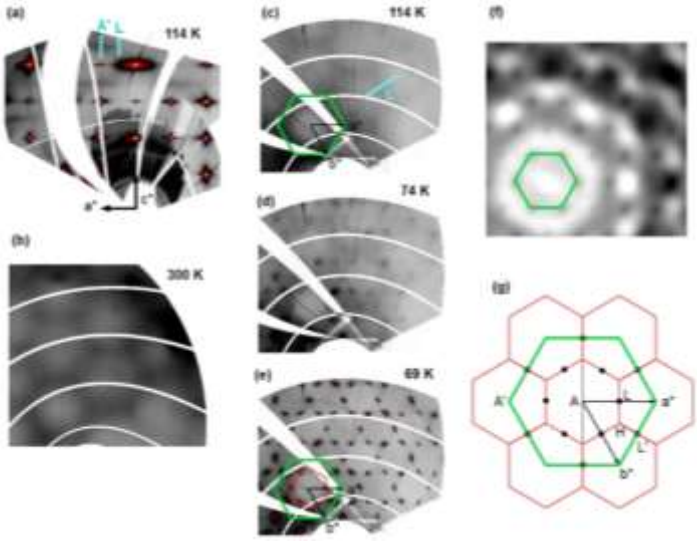

FIG. 1. Reconstruction of the (h,0,l) plane at 114 K (a), and the (h,k, 3.5) plane at 300 K (b), 114 K (c), 74 K (d), and 69 K (e). Calculated TDS intensity, including only inelastic contribution and corresponding to the Cmc21 space group is shown in (f). It should be compared to the diffuse scattering (DS) map in (c). The first Brillouin zone (BZ), six shifted first BZ covering a part of the second BZ (red lines), and a diffuse hexagon (green line) are schematically shown in (g). High-symmetry points Gamma, A, H, L, are indicated in the first BZ. A′ and L′ are the equivalent points out of the first BZ. Black full (open) circles show the positions of the satellites in the first (shifted first) BZ, which are L (L′) points, respectively. The first BZ and a diffuse hexagon are shown in (e), while solely a diffuse hexagon position is given in (c) and (f). Light blue lines in (a) and (c) indicate line scans in DS maps. Points A′ (diffuse hexagon corner) and L are scanned in the c∗ direction in (a), while L′ is scanned in the a∗+b∗ direction in (c). The analysis of the scans is presented in Fig.4. Unit cell wave vectors are given in hexagonal

2- Inelastic X-ray scattering

a- Phonon dispersion

Figure 2(a) shows the phonon dispersion measured by IXS. In the energy range 0–15 meV, there are two phonons bands: the low-energy phonon is indicated by red points, and the high-energy phonon by black triangles. The path followed along high-symmetry lines is indicated in Fig.2(b). The phonon energy shows very small variations besides Gamma-A, A-L, and A'-L lines. Note that in A', the high-energy phonon has negligible intensity. Moreover, in A, the low-energy phonon has two components. The low-frequency phonon spectrum is strongly perturbed in the vicinity of the Gamma point because of the instability leading to the hexagonal to or-thorhombic transition. The calculations on the orthorhombic structure show that the phonons in the 0–15 meV energy range are essentially dispersion less besides when approaching the Gamma point.

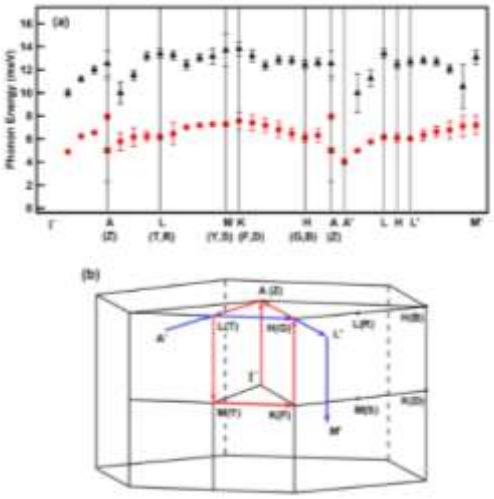

FIG. 3. (a) q dependence of the energy of the two phonons along high-symmetry lines, measured at 75 K. High-symmetry points are indicated for the hexagonal (orthorhombic) BZ. (b) The first BZ withthe explored high-symmetry lines,-A-L-M-K-H-A (red arrows). Additional path is explored out of the first BZ, A′-L-H-L′-M′(bluearrows), where edges of diffuse hexagons appear. Note that the posi-tions of the points, M, K, M′ are not exact, but there is an error of 5% of the reduced wave vector in the hand k directions. Moreover, in the orthorhombic phase, at least 3 twins coexist. A general q point in experimental data becomes a superposition of nonequivalent points of the reciprocal orthorhombic unit cell. For example, the L point inthe hexagonal phase becomes a superposition of T and R points in the orthorhombic phase.

b- <u>Temperature evolution</u>

We have studied the IXS energy scans at different temperatures on L, L', and A' points, corresponding to the two satellites and the hexagon-diffuse corner. We found that the phonon energy does not change with temperature. We can note that on cooling, the central peak (CP) intensity, mostly larger than the (LE, HE) phonon intensity, increases for L and L', and decreases for the A'point. Temperature dependence of the energy position and the HWHM of the two phonon responses are given in Figs.3(a) and 3(b). The energy of the two phonons at the two satellite positions does not decrease when the temperature approaches the MI transition: there is clearly no phonon softening. Moreover, the width of the low-energy phonon only slightlyincreases on approaching the MI transition. From these data it is clear that there is no Kohn anomaly at the critical wave vector associated with the MI transition. The Peierls transition in BaVS3 is not phonon driven. Its characteris not displacive, but of order-disorder type.

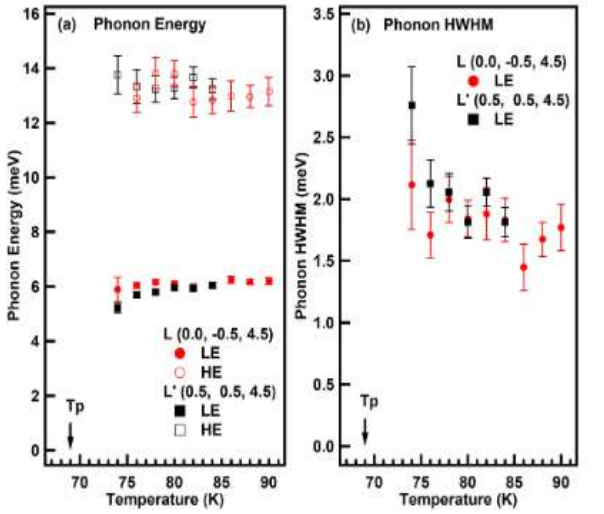

FIG. 3. Temperature evolution of the phonon (a) energy, (b) HWHM, measured at the two satellite positions. The error bars ofthe HWHM of the high-energy phonon being too large, the data arenot shown.

These results have been published : Vita Ilakovac *et al.* Order-disorder type of Peierls instability in BaVS3, PHYSICAL REVIEW B 103, 014306 (2021)